

Accepted Manuscript

Facile one-pot strategy to prepare Ag/Fe₂O₃ decorated reduced graphene oxide nanocomposite and its catalytic application in chemoselective reduction of nitroarenes

Bappi Paul, Debraj Dhar Purkayastha, Siddhartha Sankar Dhar, Subhankar Das, Sudipta Haldar

PII: S0925-8388(16)31207-5

DOI: [10.1016/j.jallcom.2016.04.229](https://doi.org/10.1016/j.jallcom.2016.04.229)

Reference: JALCOM 37427

To appear in: *Journal of Alloys and Compounds*

Received Date: 23 February 2016

Revised Date: 6 April 2016

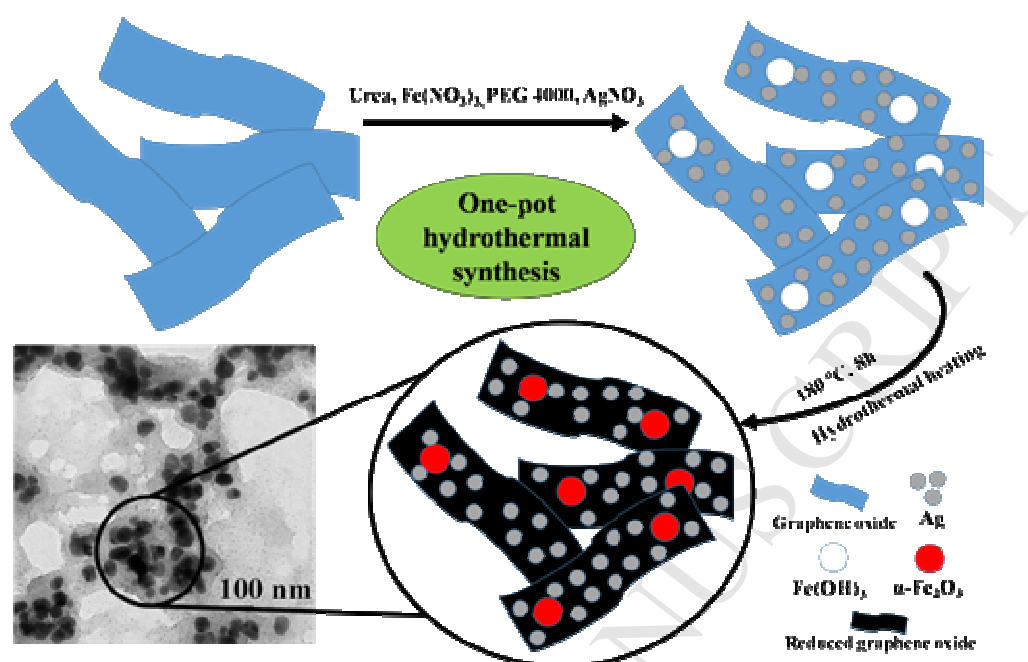
Accepted Date: 22 April 2016

Please cite this article as: B. Paul, D.D. Purkayastha, S.S. Dhar, S. Das, S. Haldar, Facile one-pot strategy to prepare Ag/Fe₂O₃ decorated reduced graphene oxide nanocomposite and its catalytic application in chemoselective reduction of nitroarenes, *Journal of Alloys and Compounds* (2016), doi: [10.1016/j.jallcom.2016.04.229](https://doi.org/10.1016/j.jallcom.2016.04.229).

This is a PDF file of an unedited manuscript that has been accepted for publication. As a service to our customers we are providing this early version of the manuscript. The manuscript will undergo copyediting, typesetting, and review of the resulting proof before it is published in its final form. Please note that during the production process errors may be discovered which could affect the content, and all legal disclaimers that apply to the journal pertain.



Graphical abstract



One pot in-situ synthesis of $\text{Ag}/\text{Fe}_2\text{O}_3$ anchored rGO assisted by urea and PEG 4000 is described. The novel nanohybrid material ($\text{Ag}/\text{Fe}_2\text{O}_3$ -rGO) is used as highly efficient magnetically separable heterogeneous catalyst for chemoselective reduction of nitroarenes to corresponding amines.

1 **Facile one-pot strategy to prepare Ag/Fe₂O₃ decorated reduced graphene oxide**
2 **nanocomposite and its catalytic application in chemoselective reduction of nitroarenes**

3 Bappi Paul^a, Debraj Dhar Purkayastha^a, Siddhartha Sankar Dhar^{a*}, Subhankar Das^b, Sudipta Haldar^b

4 ^aDepartment of Chemistry, National Institute of Technology Silchar, Silchar-788010, Assam, India

5 ^bDepartment of Mechanical Engineering, National Institute of Technology Silchar, Silchar-788010,

6 Assam, India

7 *Corresponding authors. Tel: +91-03842-242915; fax: +91-03842-224797

8 Email:ssd_iitg@hotmail.com (S.S. Dhar)

9 **Abstract**

10 The present work reports about one-pot hydrothermal synthesis of a composite of Ag/Fe₂O₃
11 anchored on reduced graphene oxide (rGO) via homogeneous chemical precipitation of
12 Fe(OH)₃ and simultaneous reduction of Ag(I). The pristine aqueous suspension of graphene
13 oxide (GO) synthesized by Hummers method is mixed with Fe(NO₃)₃·9H₂O, AgNO₃, urea and
14 polyethylene glycol (PEG 4000). The mixture under hydrothermal conditions transforms into
15 Ag/α-Fe₂O₃-rGO nanohybrid. Here PEG 4000 plays dual role of surfactant as well as reducing
16 agent for Ag(I). The synthesized Ag/Fe₂O₃-rGO nanocomposite was used as magnetically
17 recoverable catalyst for room-temperature chemoselective reduction of aromatic nitro groups to
18 the corresponding amines.

19 **Keywords:** Reduced graphene oxide; Magnetic catalyst; Nitroarenes; Chemoselective.

20 **1. Introduction**

21 Selective reduction of aromatic nitro compounds to amines is one of the highly useful organic
22 transformations[1]. Functionalized aromatic amines are important feedstock for the synthesis of
23 agrochemicals, dyes, pharmaceuticals, polymers, and various other industrially important fine
24 chemicals[2-4]. In industry, the reduction of nitroaromatics is carried out in the gas phase using a

25 nickel, copper or iron catalyst in the presence of various hydrogen sources[5,6]. The most
26 commonly used method for the production of aromatic amines is the reduction of corresponding
27 nitro substrates, using stoichiometric amounts of reducing agents. However, these traditional
28 noncatalytic processes are environmentally non-sustainable because of generation of the large
29 amount of waste[6-8]. Homogenous catalysts generally dissolve in reaction media, thus
30 providing more readily-accessible active catalytic sites, which results in mild reaction conditions
31 and good selectivity. These catalysts, however, have limited usages due to problems in
32 separating the products contaminated with unstable residues as well as recycling of the expensive
33 catalysts[9]. Whereas the catalytic reductions of nitro groups in the presence of metal complexes,
34 metal sulfides or metal powder have various practical drawbacks, such as toxic by-products and
35 inefficient reusability[4,10-12]. Magnetic nanoparticles (NPs) can play a dual role in serving
36 both as catalysts as well as magnetic carriers of catalysts. Noble metal NPs possess fascinating
37 physicochemical properties and their catalytic activities have been extensively explored in recent
38 times. However, these NPs tend to aggregate due to their high surface energy during reaction
39 which eventually diminish their catalytic activity[13]. Industrial applications of these NPs are
40 also limited due to their high cost and poor recoverability from the reaction medium. These
41 problems are usually overcome by immobilizing noble metal NPs of specific shapes and sizes on
42 various solid supports[14-16]. Among the solid supports, magnetic NPs and porous carbon
43 materials have received great attention in recent past[17-18]. Magnetic nanoparticles are easy to
44 separate from the reaction medium by use of external magnet while carbon materials possess
45 high specific surface area. The combination of these types of materials may significantly can
46 further improve activity and dispersibility of noble metal NPs[19-22]. Recently, heterodimeric
47 nanocrystals with noble metals and iron oxides have been synthesized and used as magnetic

48 reusable catalyst. Park and co-workers synthesized Au-Fe₃O₄ heterodimer nanocatalysts and
49 applied them for the chemoselective reduction of nitro compounds[23]. Jang et al. reported a
50 simple and one pot synthesis of Rh-Fe₃O₄ heterodimer nanocatalyst and demonstrated their
51 application as magnetically recoverable catalyst for efficient and selective reduction of
52 nitroarenes[24]. A core-shell magnetic Fe@Au NPs anchored graphene oxide have been recently
53 reported for chemoselective and regioselective reduction of aromatic nitro group[19].
54 Recently, copper nanoparticles loaded on Fe₃O₄@SiO₂ have been designed and catalytic
55 performance was investigated in the reduction of aromatic nitro compounds[25]. Although above
56 cited noble metal supported on iron oxide magnetic nanocatalysts have various advantages, such
57 as easy recovery and good efficiency, however their activity and selectivity are affected by steric
58 and diffusion factors[6]. Therefore, such heterodimeric nanocatalysts if supported on porous
59 carbon material, the surface area is substantially increased and nanocatalyst can be evenly
60 dispersed in the pores[26]. Graphene oxide has been proven to be one of the most important
61 porous carbon supports for anchoring metal nanoparticles[27-31]. Graphene oxide possesses very
62 large specific surface area (up to 400 to 1500 m² g⁻¹) and also exhibits high utilization of its
63 surface area because both sides of its nanosheets are accessible[28,32]. Therefore, there exists a
64 great possibility of high synergistic effect between noble metals and GO, which can greatly
65 enhance the performance of the material. Ag NPs supported on various metal and metal oxides
66 nanoparticles including magnetically recoverable nanoparticles have been the subject of
67 considerable interest for past several years[33]. To the best of our knowledge, Ag supported
68 Fe₂O₃ embedded on rGO has not been reported. As a part of our ongoing research on synthesis
69 and application of nanocatalysts[34-37], herein, we report development of one-pot hydrothermal
70 synthesis of Ag/Fe₂O₃ embedded rGO and studies of its catalytic activity for room-temperature

71 chemoselective reduction of aromatic nitro groups. The morphology, structure and composition
72 of as-prepared catalyst were characterized by various analytical techniques. The catalyst showed
73 superior performance and good selectivity for reduction of nitroarenes to amines by hydrazine
74 hydrate.

75 **2. Experimental**

76 2.1 Materials and physical measurements

77 Graphite powder, ferric nitrate and silver nitrate were purchased from Sigma Aldrich. Urea and
78 PEG 4000 were purchased from Merck India Ltd. Double distilled water was used throughout
79 the experiment. FT-IR spectrum was recorded on KBr matrix with Bruker 3000 Hyperion
80 Microscope with Vertex 80 FT-IR system. Thermogravimetric analysis (TGA) was performed in
81 air on a Netzsch STA449F3 thermal analyzer maintaining flow rate of 20 mL/min and heating
82 rate of 10°C/min. XRD measurements were carried out on a Bruker AXS D8-Advance powder
83 X-ray diffractometer with Cu-K α radiation ($\lambda=1.5418\text{\AA}$) with a scan speed of 2°/min.
84 Transmission electron microscopy images were obtained on a JEOL, JEM2100 equipment. The
85 sample powders were dispersed in ethanol under sonication and TEM grids were prepared using
86 a few drops of the dispersion followed by drying in air. Nitrogen adsorption-desorption
87 isotherms were obtained with a Micromeritics ASAP 2010 surface area and porosity analyzer.
88 Magnetism of the material was studied using a Lakeshore VSM 7410 at 300 K.

89 2.2 Synthesis of Graphene Oxide

90 Graphite powder (GP) was oxidized by modified Hummers method[38,39]. In detail,
91 concentrated H₃PO₄ and concentrated H₂SO₄ were mixed in a 250 mL round bottomed flask
92 (RB), followed by addition of graphite powder. The RB was put in a preheated 50°C water bath
93 under magnetic stirring, followed by slow addition of KMnO₄ and the stirring was continued for

94 another 6 h. This was followed by addition of diluted H_2O_2 into the solution without interruption
95 until no bubbles were produced, while the color of the solution changed from black to purple and
96 finally became bright yellow. The mixture was stirred for another 3 h. The solid product thus
97 obtained was cooled to room temperature and separated by centrifuge. Product was then washed
98 with HCl (5%), alcohol, and deionized water to obtain the graphene oxide. The collected
99 sediment was dispersed in alcohol and treated ultrasonically. Subsequently, the concentration of
100 the graphene oxide suspension was calculated by weighing the mass of the sample after drying at
101 90°C for 24 h.

102 2.3 Synthesis of $\text{Ag}/\alpha\text{-Fe}_2\text{O}_3\text{-rGO}$ nanocomposite

103 An amount of 0.80 g of $\text{Fe}(\text{NO}_3)_3 \cdot 9\text{H}_2\text{O}$ (2 mmol) and 0.084 g of AgNO_3 (0.5 mmol) were added
104 to 20 mL of a 1.8 mg mL^{-1} GO aqueous solution while stirring. To this 1.08 g of urea (0.0018 M)
105 and 2 g of PEG 4000 (0.5 mmol) were added and the above mixture was sonicated for 15 min at
106 25°C . After sonication for 15 min about 80 mL deionized water was added to the resulting
107 solution and transferred into a 100 mL Teflon-lined stainless steel autoclave, and heated at 180
108 $^\circ\text{C}$ in an electric oven for 8 h. The resulting black product was cooled to room temperature,
109 washed with deionized water and ethanol several times. Finally, the product was dried at 50°C in a
110 vacuum oven for 3 h. For comparison, bare nano $\text{Ag}/\alpha\text{-Fe}_2\text{O}_3$ material without GO was also
111 prepared under the similar condition.

112 2.4 General procedure for the room temperature reduction of nitroarenes

113 In a typical procedure, 1.0 mmol of aromatic nitro compound was slowly added to the stirred
114 aqueous suspension of 50 mg of freshly prepared nanoparticles catalysts ($\text{Ag}/\alpha\text{-Fe}_2\text{O}_3\text{-rGO}$) and
115 the contents was stirred at room temperature for about 5 min. A total of 0.2 mL of hydrazine
116 monohydrate was then added to the mixture and the reaction contents was further stirred. Stirring

117 was continued for required time (Table 2) till complete conversion was achieved. Progress of the
118 reaction was monitored by thinlayer chromatography. After completion of the reaction, the
119 catalyst was separated magnetically from the reaction mixture and the product was extracted by
120 ethyl acetate (3×5 mL).The organic layer was dried over anhydrous Na₂SO₄ and filtered off, and
121 the solvent was evaporated at reduced pressure. All of the products were characterized by ¹H
122 NMR (400 MHz with TMS as the standard).

123 **3. Results and Discussion**

124 Synthesis of a composite of Ag/Fe₂O₃ anchored on rGO has been successfully achieved by
125 hydrothermal heating of a ferric hydroxide (Fe(OH)₃) precursor obtained by a homogeneous
126 chemical precipitation and simultaneous reduction of Ag(I) (Scheme 1). Here, urea was used for
127 hydroxylation. Urea decomposes at the experimental temperature to NH₃ and CO₂. NH₃
128 combines with water to produce ammonium (NH₄⁺) and hydroxide (OH⁻) ions. Here, hydroxide
129 anions are produced by hydration of urea, which cause a uniform rise in pH of the solution till
130 the solubility limit. The free OH⁻ ions then combines with Fe³⁺ ions forming Fe(OH)₃. It is
131 pertinent to mention here that polyethylene glycol (PEG) with uniform and ordered chain
132 structure can act as a very useful surfactant to control size and morphology of the nanomaterials.
133 Normally for reduction of GO to rGO, a reducing agent such as sodium borohydride, aluminium
134 hydride, hydrohalic acid, hydrazine etc. is required, but the main advantage of using urea lies in
135 the fact that no extra reducing agent is required. In the present synthesis, hydroxylating agent
136 urea also served as reducing agent for GO. Here, PEG 4000 also plays dual role as surfactant in
137 order to control the particle size, size distribution of the nanoparticles and as well as reducing
138 agent for AgNO₃.The Ag/α-Fe₂O₃ nanoparticles are grown on the surfaces of the reduced
139 grapheme oxide nanosheets through *in situ* reduction of the pristine GO under a hydrothermal

140 treatment at 180°C for 8 h. The main advantage in this process is that uniform rise in pH
141 prevents the occurrence of high local supersaturation, allowing nucleation to occur
142 homogeneously throughout the solution.

143 <Scheme 1.>

144 3.1 Catalyst characterization

145 XRD analysis of the catalyst

146 <Fig.1.>

147 The powder XRD pattern was recorded for identification of phases exhibited by the synthesized
148 material. Fig.1 shows the powder XRD pattern of the synthesized Ag/ α -Fe₂O₃-rGO
149 nanocomposite. The diffraction peaks matches well with the reported data of α -Fe₂O₃ (JCPDS
150 File no. 87-1166). α -Fe₂O₃ possess a rhombohedrally centered hexagonal structure of the
151 corundum type with a close-packed oxygen lattice in which two thirds of the octahedral sites are
152 occupied by Fe(III) ions[40]. In addition, two diffraction peaks at 2 θ values 38.19° and 44.46°
153 corresponds to (111), and (200) planes of face-centered cubic Ag (JCPDS File no. 87-0720).
154 This indicates formation of pure Ag/ α -Fe₂O₃ nanoparticles. The Ag/ α -Fe₂O₃-rGO nanocomposite
155 also showed an additional diffraction peak at 25.5° which can be attributed to (002) plane of
156 rGO. The average crystallite size of the synthesized Ag/ α -Fe₂O₃-rGO nanocomposite was
157 estimated by the Debye-Scherrer equation [34], $d = k\lambda/\beta\cos\theta$, where 'd' is the average crystallite
158 size, ' λ ' is the wavelength of Cu-K α radiation, ' β ' is the full width at half maximum (FWHM) of
159 the highest intensity diffraction peak, ' θ ' is the Bragg diffraction angle and 'k' is the shape
160 factor, whose value is about 0.9. The average crystallite size of the synthesized Ag/ α -Fe₂O₃-rGO
161 nanocomposite was found to be 25.1 nm.

162 TEM and EDS analysis of the catalyst

163 <Fig.2.>

164 The TEM image of the synthesized Ag/ α -Fe₂O₃-rGO nanocomposite is shown in Fig.2. From the
165 TEM image it can be seen that the α -Fe₂O₃ and Ag nanoparticles are distributed homogeneously
166 in the rGO sheets. Fig.2b shows irregularly shaped particles of α -Fe₂O₃ with diameter 10-35 nm
167 and Ag NPs of size 2-5 nm. It can be seen from Fig.S1 in ESI Ag nanoparticles are in close
168 contact with α -Fe₂O₃ nanoparticles. The spacing of the lattice fringes were found to be separated
169 by 0.251 and 0.234 nm, possibly due to (110) plane of α -Fe₂O₃ and (111) plane of metallic Ag
170 respectively. The ED pattern indicated polycrystalline nature of the material. The EDS pattern
171 (Fig.3) showed Fe, C, Ag and O, which confirms the formation of Ag/ α -Fe₂O₃-rGO
172 nanocomposite.

173 <Fig.3.>

174 Raman spectra of the catalyst

175 <Fig.4.>

176 Fig.4 shows the SERS signal of GO and Ag/ α -Fe₂O₃-rGO nanocomposite in the range of 1000-
177 1800 cm⁻¹. The materials showed two prominent peaks at 1352 and 1590 cm⁻¹, which correspond
178 to D-band (defect (D) peak) and G-band (graphite (G) peak), respectively. The values are
179 consistent with literature reports [41]. The D-band/G-band intensity ratio (I_D/I_G) of these peaks
180 provide the disorder levels of the materials. The I_D/I_G of GO and Ag/ α -Fe₂O₃-rGO
181 nanocomposite were determined to be 0.826 and 1.001, respectively. The increase in the ratio of
182 I_D/I_G of Ag/ α -Fe₂O₃-rGO was recognized due to the reduction of GO to rGO in the process of
183 synthesis of Ag/ α -Fe₂O₃-rGO.

184 TGA of the catalyst

185 <Fig.5.>

186 The TGA curves of GO and Ag/ α -Fe₂O₃-rGO nanocomposite are shown in (Fig.5 (a,b)). The
187 mass loss of 5 % at around 100-170°C which may be attributed to the removal of water molecule
188 trapped inside the GO and a maximum weight loss of 65 % in the temperature range of 170-
189 525°C may be ascribed to the pyrolysis of the labile oxygen-containing groups in the forms of
190 CO, CO₂ and steam. Ag/ α -Fe₂O₃-rGO exhibits overall weight loss of only 17% when the sample
191 was heated up to 800°C at the heating rate of 10°C per minute. This weight loss corresponds to
192 loss of residual oxygen-containing groups of rGO from Ag/ α -Fe₂O₃-rGO.

193 **N₂adsorption-desorption isotherm analysis of the catalyst**

194 <Fig.6.>

195 The N₂ adsorption-desorption isotherm of Ag/ α -Fe₂O₃-rGO nanocomposite (Fig.6) follows the
196 characteristics of a type IV isotherm with a type H₃ hysteresis loop associated with aggregates of
197 plate-like particles forming slit-like pores [42]. The material showed high BET specific surface
198 area and pore volume of 772.65(m²/g) and 1.47(cm³/g), respectively. The Barrett Joyner Halenda
199 (BJH) pore size distribution indicates that most of the pores range from 5 to 20 nm as shown in
200 inset of Fig.6.

201 **VSM analysis of the catalyst**

202 <Fig.7.>

203 The magnetic hysteresis measurement Fig.7 of Ag/ α -Fe₂O₃-rGO nanocomposite was carried out
204 at 300 K with the applied magnetic field sweeping from -20000 to +20000 G. The magnetic
205 hysteresis loops showed a ferromagnetic behavior with a remnant magnetization (M_r) of 15.13
206 emu g⁻¹ and coercivity (H_c) of 572.03 G. The saturation magnetization of Ag/ α -Fe₂O₃-rGO

207 catalyst is 57.2 emu g^{-1} . The nature of the hysteresis loop and value of saturation magnetization
208 clearly indicate strong ferromagnetic property of the nanocomposite.

209 **3.2 Catalytic activity of Ag/ α -Fe₂O₃-rGO nanocomposite for reduction of nitroarenes using**
210 **hydrazine monohydrate at room temperature.**

211 After successful synthesis and full characterization of Ag/ α -Fe₂O₃-rGO nanocomposite, we
212 examined its catalytic activity for reduction of nitroarenes to aromatic amines by hydrazine
213 hydrate. In order to get best results, the reaction variables such as solvent, and amount of catalyst
214 were optimized. For this purpose, nitrobenzene was chosen as a model substrate. The experiment
215 was conducted under different solvents *viz.* acetonitrile, dichloromethane, toluene and water. It is
216 evident from the optimization studies that water is the best solvent for the present catalytic
217 system. The reaction was also studied at different mole ratios of substrate, reducing agents and
218 catalyst (Table 1). A blank run in absence of the catalyst gives a very poor yield of the product
219 after a long reaction time.

220 <Table 1.>

221 Best results were obtained when catalyst amount is 50 mg and ratio of substrate to reducing
222 agent is 1:4. Increasing the amount of reducing agent beyond four equivalents did not improve
223 the yield significantly. To demonstrate the scope of the catalyst, a range of aromatic nitro
224 compounds were reduced to corresponding amines employing optimized reaction conditions and
225 the results are summarized in Table 2. Expectedly nitroarenes with both electron withdrawing as
226 well as electron donating functional groups, afforded good to excellent yields. All the products
227 were characterized by IR spectroscopy and melting point determination. To ascertain the role of
228 the catalyst, we have prepared Ag NPs and α -Fe₂O₃ NPs separately using our reported
229 methods[34,35] and used them separately as catalyst for reduction of nitroarenes to aromatic
230 amines and observed that independently they also show catalytic activity but efficiency is

231 significantly less compared to the nanocomposite. We then mixed these NPs (Ag NPs and α -
232 Fe_2O_3 NPs) at room temperature and used this mixture as catalysts for reduction of nitroarenes
233 but we have not seen any improvement of the yield of the product. The $\text{Ag}/\alpha\text{-Fe}_2\text{O}_3$ (Ag
234 supported $\alpha\text{-Fe}_2\text{O}_3$) was also synthesized and used as catalysts but some improvement in the
235 catalytic performance was observed but still no way comparable to the performance of the $\text{Ag}/\alpha\text{-Fe}_2\text{O}_3\text{-rGO}$
236 nanocomposite. This clearly indicates Ag NPs and $\alpha\text{-Fe}_2\text{O}_3$ NRs in isolation, a simple
237 random mixture of these components as well as $\text{Ag}/\alpha\text{-Fe}_2\text{O}_3$ have significantly lower catalytic
238 effect on reduction of nitroarenes. Therefore it can be concluded that role of rGO as a support in
239 $\text{Ag}/\alpha\text{-Fe}_2\text{O}_3\text{-rGO}$ is very important in enhancing the performance of the composite catalyst. A
240 comparison between the present catalyst and some of the previously reported catalytic methods
241 for reduction of nitroarenes to aromatic amines is summarized in Table 3. The comparison reveals
242 that catalytic reaction presented herein is better than to the some of the most efficient catalytic
243 reductions of aromatic nitroarenes to amines. The added advantage of the present catalyst is its
244 easy recovery and recyclability.

245 <Table 2.>

246 <Table 3.>

247 3.3. Recyclability of the catalyst

248 After completion of the reaction, the solid catalyst was separated magnetically from the reaction
249 mixture and washed thoroughly with acetone and reused for multiple cycles to check the
250 efficiency of the recycled catalyst. The catalytic reduction of nitroarenes to aromatic amines was
251 carried out with the reused catalyst under the same reaction condition. The activity of the
252 recovered catalyst after 5 consecutive runs did not show any significant decline (Fig.8). The
253 TEM image of the spent catalyst showed an almost similar size and shape to that of the fresh
254 catalyst (Fig.S2 in ESI). Leaching test has been carried out by procedure reported [41]. To

255 confirm that there is no leaching of Ag particles during the reaction, we have removed the
256 catalyst magnetically after 15 min of the reaction. The yield of the product obtained at 15
257 minutes was noted. The reaction was further continued without the catalyst for another 15
258 minutes but we did not observe any increase in the yield. Since Ag is one of the catalytically
259 active components of the composite, so if there had been leaching of Ag NPs, we would have
260 observed some rise in yield. Therefore it can be stated that there is no leaching of Ag NPs from
261 the Ag/ α -Fe₂O₃-rGO catalyst during the reaction.

262 <Fig.8.>

263 4. Conclusion

264 In summary Ag/ α -Fe₂O₃-rGO nanocomposite has been successfully synthesized by the one-pot
265 hydrothermal method. The role of urea as hydroxylating agent and PEG 4000 as surfactant as
266 well as reducing agent are important features of the synthesis method. This novel
267 nanocomposite, Ag/ α -Fe₂O₃-rGO, is used as recyclable catalyst in reduction of range of aromatic
268 nitroarenes to amines. To the best of our knowledge, such rGO embedded nanocomposite has not
269 been previously used for conversion of nitroarenes to amines. This catalytic protocol has various
270 advantages such as high yields, elimination of homogeneous catalysts, simple work-up and easy
271 separation and recycling of the catalyst. The catalyst also shows true heterogeneity as its
272 efficiency remains almost the same after five cycles of reuse.

273 Acknowledgement

274 The authors thank SAIF, IIT Madras, SAIF, IIT Bombay and SAIF, North Eastern Hill
275 University for analysis. The Director NIT Silchar is acknowledged for financial support.

276 References

277 [1] D. Cantillo, M. M. Moghaddam, C.O. Kappe, *J. Org. Chem.* 78 (2013) 4530-4542.

- 278 [2] R.S. Downing, P.J. Kunkeler, H.V. Bekkum, *Catal. Today*. 37 (1997) 121-136.
- 279 [3] N. Ono, Wiley-VCH: New York, 2001.
- 280 [4] R.K. Rai, A. Mahata, S. Mukhopadhyay, S. Gupta, P. Li, K.T. Nguyen, Y. Zhao, B.
281 Pathak, S.K. Singh, *Inorg. Chem.* 53 (2014) 2904-2909.
- 282 [5] O. Verho, K.P.J. Gustaffson, A. Nagendiran, C.W. Tai, J.E. Backvall, *Chem. Cat. Chem.* 6
283 (2014) 3153-3159.
- 284 [6] M. Shokouhimehr, *Catalysts*. 5 (2015) 534-560.
- 285 [7] S. Nishimura, Wiley-Interscience: New York, 2001.
- 286 [8] H. Arnold, F. Dobert, J. Gaube, Wiley-Interscience: New York, 2008, 3266-3284.
- 287 [9] C. Coperet, M. Chabanas, R.P.S. Arroman, J.M. Basset, *Angew. Chem. Int. Ed.* 42
288 (2003) 156-181.
- 289 [10] R. Barden, H. Knupfer, S. Hartung, U.S. Patents 4,002,673.
- 290 [11] G. Weinhofer, M. Baseda-Kruger, C. Ziebart, F. A. Westerhaus, W. Baumann, R. Jackstell,
291 K. Junge, M. Beller, *Chem. Commun.* 49 (2013) 9089-9091.
- 292 [12] G. Wienhofer, I. Sorribes, A. Boddien, F. Westerhaus, K. Junge, H. Junge, R. Llusar, M.
293 Beller, *J. Am. Chem. Soc.* 133 (2011) 12875-12879.
- 294 [13] D. Astruc, F. Lu, J.R. Aranzaes, *Angew. Chem. Int. Ed.* 44 (2005) 7852-7872.

- 295 [14] D. Wang, D. Astruc, *Chem. Rev.* 144 (2014) 6949-6985.
- 296 [15] F. Zaera, *Chem. Soc. Rev.* 42 (2013) 2746-2762.
- 297 [16] P. Lara, K. Philippot, *Catal. Sci. Technol.* 4 (2014) 2445-2465.
- 298 [17] V. Polshettiwar, R. Luque, A. Fihri, H. Zhu, M. Bouhrara, J.M. Basset, *Chem. Rev.* 111
299 (2011) 3036-3075.
- 300 [18] D. Li, R.B. Kaner, *Science.* 320 (2008) 1170-1171.
- 301 [19] V.K. Gupta, N. Atar, M.L. Yola, Z. Ustundag, L. Uzun, *Water Res.* 48 (2014) 210-217.
- 302 [20] Z. Zhang, S. Zhai, M. Wang, H. Ji, L. He, C. Ye, C. Wang, S. Fang, H. Zhang, *J. Alloys*
303 *Compd.* 659 (2016) 101-111.
- 304 [21] A. Liu, W. Zhou, K. Shen, J. Liu, X. Zhang, *RSC Adv.* 5 (2015) 17336-17342.
- 305 [22] J.M. Thomas, B.F.G. Johnson, R. Raja, G. Sankar, P.A. Midgley, *Acc. Chem. Res.* 36
306 (2003) 20-30.
- 307 [23] S. Park, I.S. Lee, J. Park, *Org. Biomol. Chem.* 11 (2013) 395-399.
- 308 [24] Y. Jang, S. Kim, S.W. Jun, B.H. Kim, S. Hwang, I.K. Song, B.M. Kim, T. Hyeon, *Chem.*
309 *Commun.* 47 (2011) 3601-3603.
- 310 [25] M. Rajabzadeh, H. Eshghi, R. Khalifeh, M. Bakavoli, *RSC Adv.* 6 (2016) 19331-19340.
- 311 [26] M. Zhu, G. Diao, *Nanoscale.* 3 (2011) 2748-2767.

- 312 [27] B. Pant, P.S. Saud, M. Park, S. Park, H.Y. Kim, *J. Alloys Compd.* 671 (2016) 51-59.
- 313 [28] R. Nie, J. Wang, L. Wang, Y. Qin, P. Chen, Z. Hou, *Carbon*. 50 (2012) 586-596.
- 314 [29] H. Liu, T. Lv, Z. Zhu, *J. Mol. Catal. A: Chem.* 404-405 (2015) 178-185.
- 315 [30] C.K. Chua, M. Pumera, *Chem. Soc. Rev.* 43 (2014) 291-312.
- 316 [31] W.H. Lee, J. Park, S.H. Sim, S. Lim, K.S. Kim, B.H. Hong, K. Cho, *J. Am. Chem. Soc.*
317 133 (2011) 4447-4454.
- 318 [32] N.M. Khusayfan, *J. Alloys Compd.* 666 (2016) 501-506
- 319 [33] S. Ghosh, S.S. Acharyya, D. Tripathi, R. Bal, *J. Mater. Chem. A*. 2 (2014) 15726-15733.
- 320 [34] B. Paul, B. Bhuyan, D.D Purkayastha, S.S Dhar. *Catal. Commun.* 69 (2015) 48-54.
- 321 [35] B. Paul, B. Bhuyan, D.D. Purkayastha, S. S. Dhar, *J. Photochem. Photobiol. B* 154 (2016)
322 1-7.
- 323 [36] B. Paul, B. Bhuyan, D.D. Purkayastha, S.S. Dhar, S. Behera, *J. Alloys Compd.* 648 (2015)
324 629-635.
- 325 [37] B. Paul, B. Bhuyan, D.D. Purkayastha, S. S. Dhar, *J. Mol. Liq.* 212 (2015) 813-817.
- 326 [38] W.S. Hummers, R.E. Offeman, *J. Am. Chem. Soc.* 80 (1958) 1339.
- 327 [39] H.L. Poh, F. Sanek, A. Ambrosi, G. Zhao, Z. Sofer, M. Pumera, *Nanoscale*, 4 (2012) 3515-
328 3522.

- 329 [40] R. Zboril, M. Mashlan, D. Petridis, Chem. Mater. 14 (2002) 969-982.
- 330 [41] J. Wang, S.A. Kondrat, Y. Wang, G.L. Brett, C. Giles, J.K. Bartley, L. Lu, Q. Liu, C.J.
331 Kiely, G.J. Hutchings, ACS Catal. 5 (2015) 3575-3587.
- 332 [42] F.Z. Mou, J.G. Guan, Z.D. Xiao, Z.G. Sun, W.D. Shi, X.A. Fan, J. Mater. Chem. 21
333 (2011) 5414-5421.
- 334 [43] X.B. Lou, L. He, Y. Qian, Y.M. Liu, Y. Cao, K.N. Fan, Adv. Synth. Catal. 353 (2011) 281-
335 286.
- 336 [44] M.B. Gawande, A.K. Rathi, P.S. Branco, I.D. Nogueira, A. Velhinho, J.J. Shrikhande, U.U.
337 Indulkar, R.V. Jayaram, C.A.A. Ghumman, N. Bundaleski, O.M.N.D. Teodoro, Chem. Eur.
338 J. 18 (2012) 12628-12632.
- 339 [45] A.J. Amali, R.K. Rana, Green Chem. 11 (2009) 1781-1786.
- 340 [46] Y. Gao, D. Ma, C. Wang, J. Guan, X. Bao, Chem. Commun. 47 (2011) 2432-2434.
341

342 **Scheme caption**

343 **Scheme 1.** Synthesis of Ag/ α -Fe₂O₃-rGOnanocomposite.

344 **Figure captions**

345 **Fig.1.** Powder XRD pattern of Ag/ α -Fe₂O₃-rGOnanocomposite.

346 **Fig.2.** (a, b) TEM images (c) HRTEM image and (d) ED pattern of Ag/ α -Fe₂O₃-rGO
347 nanocomposite.

348 **Fig 3.** EDS pattern of Ag/ α -Fe₂O₃-rGOnanocomposite.

349 **Fig.4.** Raman spectra of GO and Ag/ α -Fe₂O₃-rGOnanocomposite.

350 **Fig.5.** TGA curve of (a) GO and (b) Ag/ α -Fe₂O₃-rGOnanocomposite.

351 **Fig.6.** (a, b) N_2 adsorption-desorption isotherms of Ag/ α - Fe_2O_3 -rGOnanocomposite.

352 **Fig.7.** Room temperature magnetization hysteresis loop of Ag/ α - Fe_2O_3 -rGOnanocomposite.

353 **Fig.8.** Catalytic activity of Ag/ α - Fe_2O_3 -rGO nanocomposite against number of cycles.

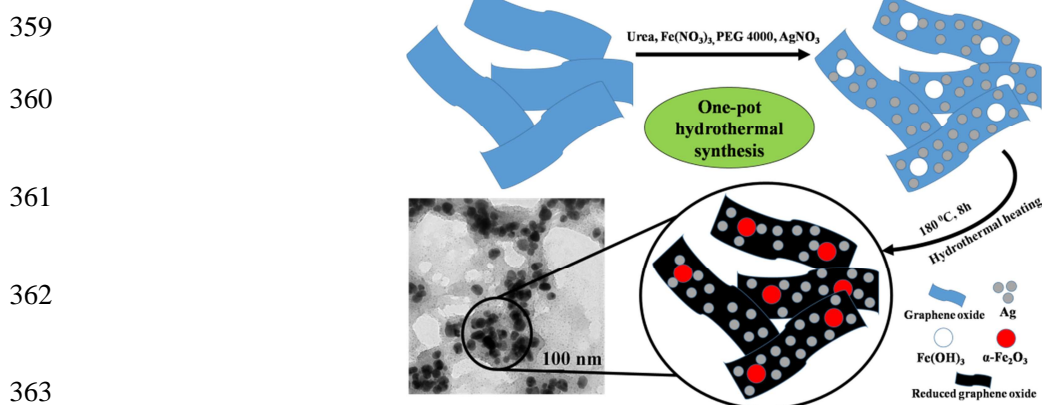
354 **Table captions**

355 **Table 1.** Optimization of reduction of nitroarenes.

356 **Table 2.** Reduction of nitroarenes in presence of Ag/ α - Fe_2O_3 -rGO catalyst.

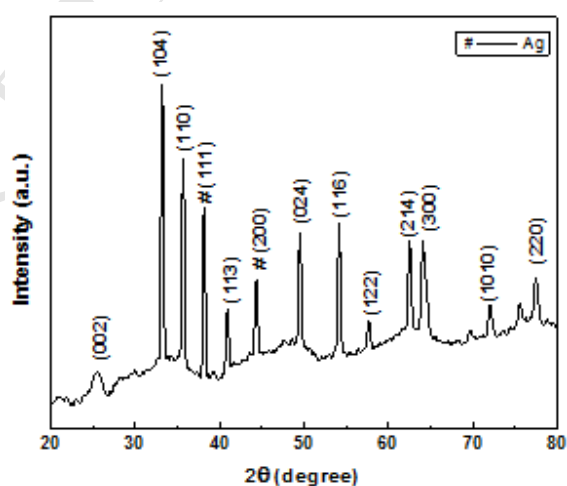
357 **Table 3.** Comparison of the literature reported catalyst with the present catalyst.

358

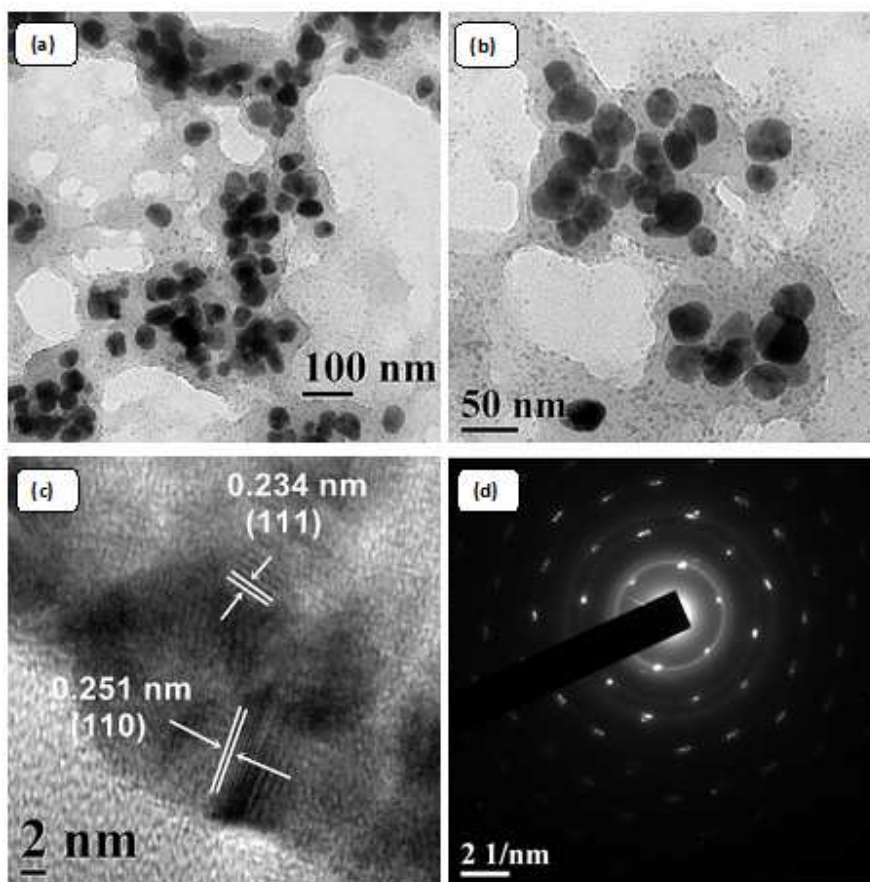


364

<Scheme 1.>



<Fig.1.>

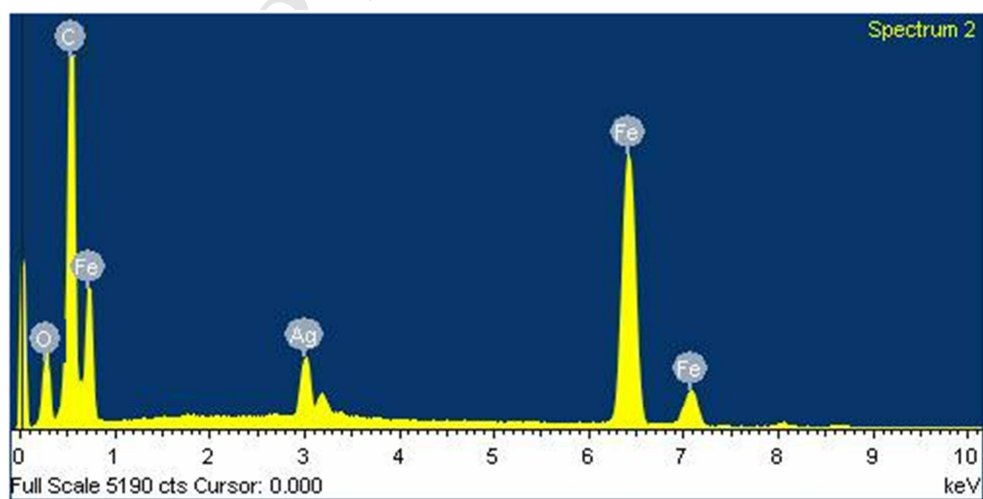


367

368

369

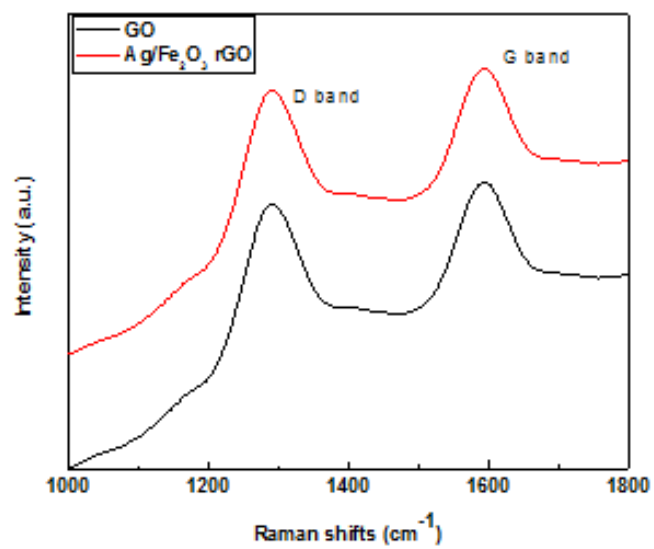
<Fig.2.>



370

371

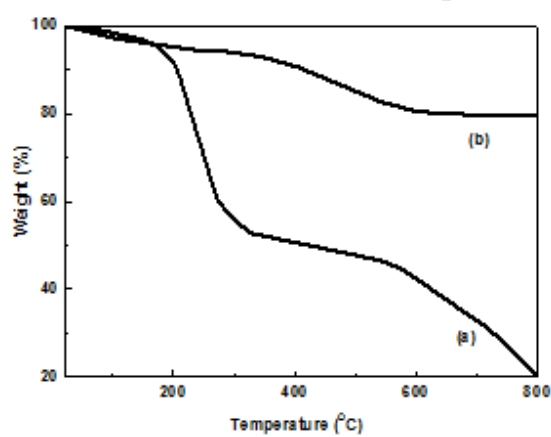
<Fig.3.>



372

373

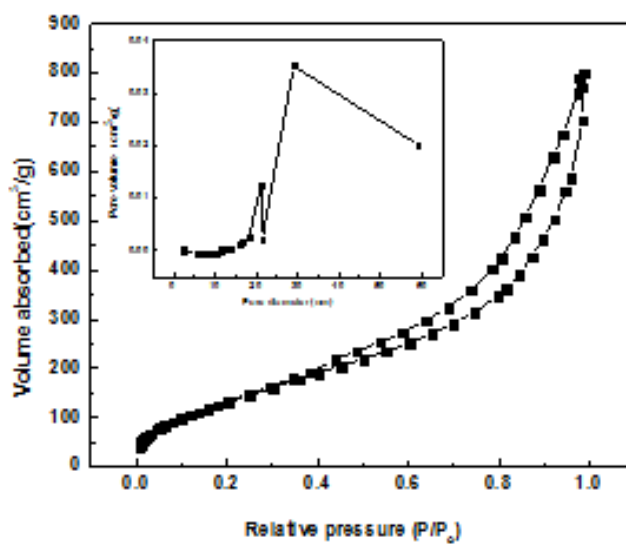
<Fig.4.>



374

375

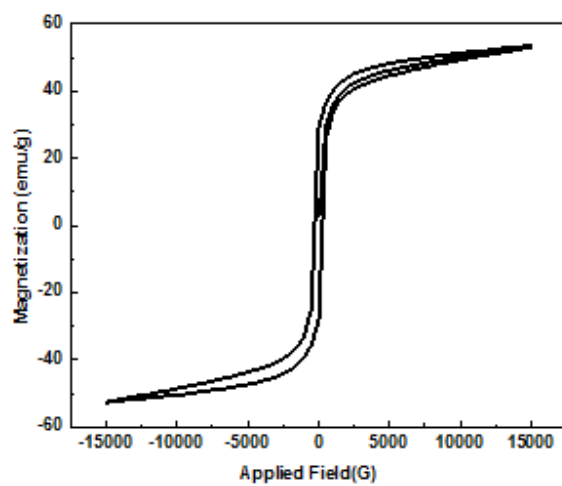
<Fig.5.>



376

377

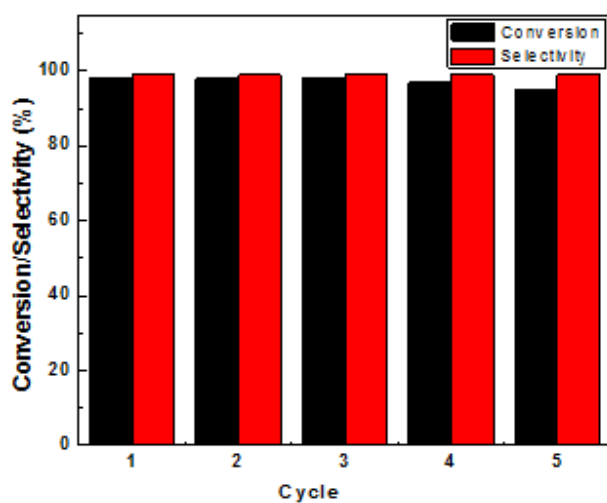
<Fig.6.>



378

379

<Fig.7.>



380

381

<Fig.8.>

382 **Table 1.**

Entry	Substrate (equiv)	Catalyst (mg)	Reducing agent (equiv)	Time(min)	Temperature (°C)	Yield(%)
1	1	100	4	60	27	95
2	1	50	8	60	27	96
3	1	50	4	15	27	98
4	2	50	4	60	27	76
5	1	30	4	60	70	92
6	1	50	4	60	80	76

383

384

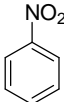
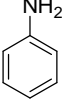
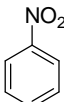
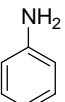
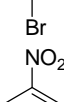
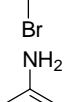
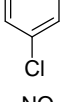
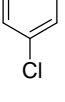
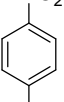
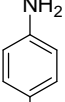
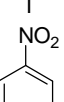
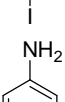
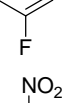
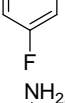
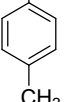
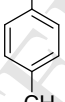
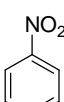
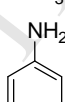
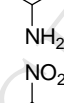
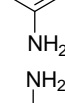
385

386

387

388

389 **Table2.**

Entry	Substrate	Product	Time (min)	Yield (%)	Selectivity(%)
1			30	98	>99
2			25	98	>99
3			45	97	>99
4			30	95	>99
5			20	98	>99
6			60	95	>99
7			30	99	>99
8			45	92	>99
9			40	95	>99
10			90	92	>99

390

391

392 **Table 3.**

Entry	Catalyst	Solvent	Temp °C	Time (min)	Yield/conversion (%)	Ref
1	Ni NPs	Water	rt	75	99 conversion	4
2	Co NPs	Water	rt	300	50 conversion	4
3	Au/TiO ₂	EtOH	rt	180	99 conversion	43
4	Ni-Fe ₃ O ₄	Glycerol	80	180	94 yield	44
5	Au-Fe ₃ O ₄	EtOH	rt	10	GC yield 99	23
6	Rh-Fe ₃ O ₄	EtOH	80	60	99 yield	24
7	Pd-Fe ₃ O ₄	EtOH	rt	60	90 yield	45
8	Fe ₃ O ₄ @SiO ₂ /EP.EN.EG@Cu	Water	rt	15	85 yield	25
9	Reduced graphene oxide	N ₂ H ₄ .H ₂ O /H ₂ O	30	2880	97 yield	46
10	Ag/ α -Fe ₂ O ₃ -rGO	Water	rt	30	98 yield	Present Work

393

394

395

396

397

398

Highlights

- One pot in-situ synthesis of Ag/Fe₂O₃ anchored rGO.
- PEG 4000 as surfactant and reducing agent for Ag(I).
- Formation of Ag/Fe₂O₃-rGO is confirmed by TEM, XRD, EDS and Raman spectroscopy.
- As-synthesized novel material exhibits pronounced activity as magnetic catalyst.
- The catalyst used for chemoselective reduction of aromatic nitro groups.